Reactive oxygen species–mitochondria pathway involved in FV-429-induced apoptosis in human hepatocellular carcinoma HepG2 cells

Zhen Yang, Lei Qiang, Tian Wu, Fei-Hong Chen, Hui-Ying Yang, Qing Zhao, Mei-Juan Zou, Ya-Jing Sun, Zhi-Yu Li and Qing-Long Guo

FV-429 is a newly synthesized flavonoid with a bis(2-hydroxyethyl) amino propoxy substitution. In this study, we investigate the anticancer effect of FV-429 both *in vivo* and *in vitro*. These data have shown that FV-429 could significantly inhibit tumor growth in mice inoculated with Heps hepatoma cells without evident toxicity. After the treatment of FV-429 (40 mg/kg), the inhibitory rate of tumor weight was 52.12%. Then, we performed diamidinophenylindole staining and annexin V/propidium iodide double-staining assay to investigate the apoptosis induced by FV-429 in HepG2 cells. Further research revealed that FV-429 induced apoptosis through the mitochondrial apoptotic pathway, as indicated by a change in Bax/Bcl-2 ratios, collapse of mitochondrial membrane potential, the transposition of apoptotic-inducing factor and cytochrome *c*, caspase-3 and caspase-9 activation, and degradation of poly (ADP-ribose) polymerase. The accumulation of reactive oxygen species induced by FV-429 in HepG2 cells was also observed. Moreover, the mitogen-activated protein kinases, the downstream effect of reactive oxygen species accumulation including c-Jun N-terminal kinase and p38 mitogen-activated protein kinases, could be activated by FV-429. Taken together, our results provided a mechanistic framework for further exploration of FV-429 as a novel chemotherapy for human tumors. *Anti-Cancer Drugs* 22:886–895 © 2011 Wolters Kluwer Health | Lippincott Williams & Wilkins.

Correspondence to Dr Qing-Long Guo, Jiangsu Key Laboratory of Carcinogenesis and Intervention, China Pharmaceutical University, 24 Tongjiaxiang, Nanjing, Jiangsu 210009, PR China
Tel/fax: + 86 25 83271055; e-mail: anticancer_drug@yahoo.com.cn

Zhen Yang and Lei Qiang contributed equally to this study.

Introduction

Liver cancer or hepatic cancer is the third most common cause of death from cancer and the sixth most common incident cancer in China, and its incidence is rising not only in China but also in many other countries [1]. It is usually treated by surgical resection or liver transplantation, with curative options for the patients when the disease is diagnosed at an early stage [2]. However, approximately 70% of patients are inoperable because of advanced tumor growth or liver cirrhosis, or, alternatively, the hepatic cancer belongs to the group of cancers that are resistant to systemic chemotherapies, radiation therapy, and even immunotherapy [3]. Novel therapeutic drugs accordingly are needed to improve the efficacy in treating hepatic cancer.

Flavonoids are a group of compounds widely distributed in plant sources, such as seeds, citrus fruits, olive oil, and tea and red wine. It has long been recognized that flavonoids possess anti-inflammatory, antioxidant, anti-allergic, hepatoprotective, antithrombotic, and antiviral activities [4]. In recent years, the antitumor effects of flavonoids have been widely recognized and studied. For instance, wogonin, a flavonoid originated from the root of a medicinal herb *Scutellaria baicalensis Georgi*, induced apoptosis in murine sarcoma S180 by the concerted modulation of p53, Bax, and Bcl-2 genes and proteins [5,6]. Oroxylin A, a flavonoid isolated from the root of *Scutellaria baicalensis Georgi*, has been reported to possess anticancer effects on hepatic carcinoma both *in vitro* and *in vivo* [7,8]. FV-429 is a newly synthesized flavonoid with bis(2-hydroxyethyl) amino propoxy substitution (Fig. 1a). Compared with most of the flavonoid family members, FV-429 shows alkalescence and an improvement of the water solubility (Table 1). In this study, we provided evidence that FV-429 has potent antitumor activity by inducing a reactive oxygen species (ROS)–mitochondrial-mediated apoptosis.

The mitochondrion controls cell-life activities, and it is not only the center of respiratory chain and oxidative phosphorylation, but also the center of cell apoptosis [9]. A substantial increase in ROS occurs in mitochondria-mediated pathway for damage of respiratory chain [10], inhibiting the mitochondrial electron transport chain, resulting in a subsequent release of cytochrome *c* from the mitochondrial intermembrane space to cytosol, thereby activating the caspase–cascade system and cleavage of poly (ADP-ribose) polymerase (PARP) [11,12]. It has been previously demonstrated that the

accumulation of ROS could cause the loss of mitochondrial membrane potential (MMP) and activates mitogen-activated protein kinases (MAPK) pathways, including the c-Jun N-terminal kinase (JNK) and the p38 pathways that are responsible for ROS-mediated cell apoptosis [13].

In this study, we demonstrated that FV-429 shows obvious antitumor effects *in vivo* and *in vitro*, in which apoptosis may be involved. Furthermore, we showed that in HepG2 cells treated with FV-429, ROS level and Bax/Bcl-2 ratio increased, with MMP collapse and the subsequent activation of caspase cascade. Moreover, we provided evidence that apoptosis induced by FV-429 was related with the activation of JNK and p38 MAPK

Fig. 1

FV-429 inhibits cell viability in HepG2 cells. (a) Molecular structure of FV-429 ($C_{23}H_{25}NO_7$, molecular weight = 429). (b) The inhibitory effect of FV-429 on HepG2 cells with different concentrations for 24 h. Data are shown as mean ± standard deviation ($n = 3$).

pathways. The inhibition of PI3K/Akt and NF-κB pathways may also contribute to FV-429-induced apoptosis. Taken together, our findings provide a new candidate compound, FV-429, for its potential use in liver cancer therapy.
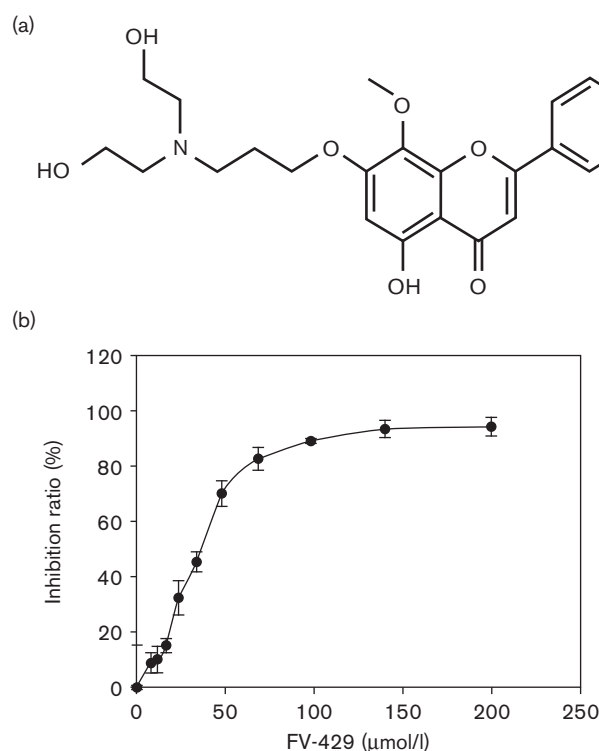
Materials and methods
Materials
FV-429, prepared in Dr Zhiyu Li's lab (China Pharmaceutical University, China), was dissolved in 100% dimethylsulfoxide (DMSO) as a stock solution, stored at $-20°C$, and diluted with medium before each experiment. Controls were always treated with the same amount of DMSO (0.1%) as used in corresponding experiments. 3-(4,5-Dimethylthiazol-2-yl)-2,5-diphenyltetrazoliumbromide (MTT) was obtained from Fluka Chemical Co. (Ronkonkoma, New York, USA), and was dissolved in 0.01 mol/l of phosphate-buffered saline (PBS). Primary antibodies of JNK, p-JNK, p38, p-p38, ERK1/2, p-ERK1/2, Bax, Bcl-2, caspase-3, procaspase-3, caspase-9, procaspase-9, Akt, p-Akt, NF-κB, histones, COX IV, and β-actin were obtained from Santa Cruz Biotechnology (California, USA). Antibodies of cytochrome *c*, apoptotic-inducing factor (AIF), and PARP were purchased from Biosource (Camarillo, California, USA) and Cell Signaling Technology (Beverly, Massachusetts, USA). Cyclosporin A was from Calbiochem (San Diego, California, USA). Carbobenzoxy-valyl-alanyl-aspartyl-[*O*-methyl]-fluoromethylketone (Z-VAD-FMK, a caspase inhibitor), *N*-acetyl-L-cysteine (NAC, the scavenger of ROS), and SB203580 (an inhibitor of p38 MAPK), SP600125 (an inhibitor of JNK) were obtained from Beyotime Institute of Biotechnology (Haimen, China).

Animals
Institute of Cancer Research species mice, weighing 18–22 g, were supplied by Experimental Animal Center, China Pharmaceutical University. Animals were housed under standard conditions at a temperature of $22°C \pm 1$ and a 12-h light–dark cycle with free access to food and water. All experiments were carried out according to the National Institutes of Health Guide for the Care and Use of Laboratory Animals (publication no. 85-23, revised 1985) and were approved by the Institutional Animal

Table 1 Effect of FV-429 on Heps in mice by intravenous route (mean ± standard deviation; $n = 10$)

| Groups | Dose (mg/kg) | Weight (g) | | Weight of tumor (g) | Inhibitory rate (%) |
		Pretreatment	Posttreatment		
Control		19.80 ± 1.48	26.90 ± 3.41*	2.01 ± 0.40	
Cyclophosphamide	20	19.50 ± 1.51	20.25 ± 3.06	0.63 ± 0.15	68.45**
	40	19.63 ± 1.30	25.00 ± 1.77*	0.96 ± 0.19	52.12**
FV-429	20	19.13 ± 1.13	26.25 ± 4.74*	1.12 ± 0.13	44.39*
	10	19.00 ± 1.07	27.63 ± 5.07**	1.39 ± 0.34	30.81*

*$P < 0.05$ vs. control.
**$P < 0.01$.

Care and Use Committee of China Pharmaceutical University.

Cells culture

The human hepatoma HepG2 cell line and human hepatocyte L02 cell line were purchased from KeyGen Biology Technology Company (Nanjing, Jiangsu, China). Cells were grown in Roswell Park Memorial Institute-1640 medium (Gibco, Grand Island, New York, USA) supplemented with 10% heat-inactivated calf serum (Sijiqing, Hangzhou, Jiangsu, China), penicillin (100 U/ml), and streptomycin (100 U/ml) in a 5% CO_2 atmosphere.

3-(4,5-dimethylthiazol-2-yl)-2,5-diphenytetrazoliumbromide assay

The HepG2 cells were plated in 96-well plates with 100 μl of cells, which had previously been resuspended to 1×10^5/ml. The cells were left to adhere overnight, and were then exposed to media and FV-429 at different concentrations for 24 h. Subsequently, 20 μl of MTT solution (5 mg/ml) was transferred to each well to yield a final assay volume of 220 μl per well. Plates were incubated for 4 h at 37°C and 5% CO_2. After incubation, supernatants were removed, and DMSO (100 μl) was added to ensure total solubility of formazan crystals. Plates were placed on an orbital shaker for 2 min, and the absorbance was recorded at 562 nm. Cell viability was determined based on mitochondrial conversion of MTT to formazan. Inhibition ratio (%) was calculated using the following equation:

$$\text{Inhibitory ratio}\,(\%) = [(A_{\text{Control}} - A_{\text{Treated}})\,/\,A_{\text{Control}}] \times 100\%$$

IC_{50} was taken as the concentration that caused 50% inhibition of cell viabilities and calculated by the Logit method [14].

Apoptosis assessment

To detect morphological evidence of apoptosis, cell nuclei were stained with the fluorescent dye diamidinophenyl-indole (DAPI). HepG2 cells, plated in six-well plates with 70–80% confluency, were treated with different concentrations of FV-429. After incubation for 24 h, cells were fixed with 4% paraformaldehyde for 20 min, and were then washed with PBS twice, followed with incubation with 0.3% TritonX-100 (in PBS) for 10 min at room temperature. After washing with PBS, the cells were incubated with DAPI (10 μg/ml) for 10 min and were then observed under fluorescence microscopy (Olympus, Japan) at an excitation wavelength of 340 nm.

Annexin V-fluorescein isothiocyanate apoptosis detection kit (BioVision Research Products, Mountain View, California, USA) assay was performed according to the manufacturer's protocol. This assay does not discriminate between apoptosis and necrosis. In brief, cells were pretreated with 1 mmol/l of NAC for 1 h, then treated with FV-429 (20, 40, and 80 μmol/l) for 24 h, and were washed with PBS. Then the cells were collected, resuspended in binding buffer [pH 7.5, 4-(2-hydro-xyethyl)-1-piperazineethanesulfonic acid (10 mmol/l), $CaCl_2$ (2.5 mmol/l), and NaCl (140 mmol/l)], and were incubated with annexin V-fluorescein isothiocyanate and propidium iodide (PI) for 10 min in the dark at room temperature; cells were analyzed by flow cytometry (FACSCalibur, Becton Dickinson, Franklin Lakes, New Jersey, USA) and a computer station running CellQuest software (BD Biosciences, Franklin Lakes, New Jersey, USA).

Mitochondrial transmembrane potential (ΔΨm) assessment

The electrical potential difference across the inner-mitochondrial membrane (ΔΨm) was monitored using the ΔΨm-specific fluorescent probe JC-1 (Molecular Probes Inc., Eugene, Oregon, USA), a sensitive fluorescent dye. In brief, the HepG2 treated with different concentrations of FV-429 (20, 40, and 80 μmol/l) for 24 h were harvested with ice-cold PBS and resuspended in Roswell Park Memorial Institute-1640 medium at a density of 0.5×10^6 cells/ml. Then the cells were washed with ice-cold PBS, incubated with 10 μmol/l of JC-1 for 15 min at 37°C in the dark, and were observed under a fluorescence microscope (Olympus IX51, Japan). Red fluorescence is attributable to a potential-dependent aggregation in the mitochondria. Green fluorescence, reflecting the monomeric form of JC-1, appeared in the cytosol after mitochondrial membrane depolarization. Relative fluorescence intensities were monitored using the flow cytometry (FACSCalibur, Becton Dickinson), and were analyzed by the software Modfit and CellQuest (BD Biosciences) with settings of FL1 (green) at 530 nm and FL2 (red) at 585 nm [15].

Measurement of reactive oxygen species formation

Generation of ROS was assessed by using the fluorescent signal 2,7-dichlorodihydrofluorescein (H_2DCFDA), a cell-permeable indicator for ROS [16]. As described previously, H_2DCFDA was oxidized to a highly green fluorescent 2,7-dichlorofluorescein by the generation of ROS. The HepG2 cells were pretreated with 20, 40, and 80 μmol/l for 10 h. The cells were incubated with H_2DCFDA (100 μmol/l) in PBS for 30 min. After 30 min at 37°C, 2,7-dichlorofluorescein fluorescence (excitation of 485 nm and emission of 525 nm) was observed under a fluorescence microscope (Olympus IX51, Japan). The fluorescence intensity was measured using flow cytometry (FACSCalibur, Becton Dickinson), and was analyzed by the software Modfit and CellQuest (BD Biosciences, Franklin Lakes, New Jersey, USA) with settings at excitation and emission equal to 488/525 nm.

Western blot analysis

After the treatment of the indicated concentration of FV-429 (20, 40, and 80 μmol/l) for 24 h, the HepG2 cells were collected and lysed in lysis buffer [Tris–Cl (100 mmol/l), pH 6.8, 4% (m/v) SDS, 20% (v/v) glycerol, β-mercaptoethanol (200 mmol/l), phenylmethanesulfonylfluoride (1 mmol/l), and aprotinin (1 g/ml)], and were measured using the bicinchoninic acid protein assay with Varioskan spectrofluorometer and spectrophotometer (Thermo; Thermo Fisher Scientific, Hudson, New Hampshire, USA) at 562 nm. The fractionation of the nuclear protein and cytoplasmic protein was performed according to the nuclear/cytoplasmic fractionation kit (Biovision Research Products) instruction. The mitochondrial and cytosolic fractions of cells were performed according to the cytosol/mitochondria fractionation kit instruction. The proteins were separated on a 10–12% SDS-polyacrylamide gel electrophoresis and were transferred onto nitrocellulose membranes. Immune complexes were formed by incubation of the corresponding antibodies for 1 h at 37°C, followed by IRDye 800-conjugated antimouse and antirabbit secondary antibodies for 1 h at 37°C. Immuno-reactive protein bands were detected with the Odyssey Scanning System (Li-COR, Nebraska, USA).

Antitumor effects in mice

The mice were transplanted with Heps cells (1×10^6 per mouse) according to protocols of transplanted tumor research. After 24 h, the mice were randomly divided into five groups containing 10 mice each. The groups with FV-429 treatment received three dosages (10, 20, 40 mg/kg), respectively. The positive group was treated with cyclophosphamide (20 mg/kg). The control group received 0.9% normal saline. All test drugs were given through injections 24 h after tumor transplantation (or inoculation). The corresponding agent for each group was administrated every day, which lasted for 9 days. At the end of treatments, all mice were killed and weighed simultaneously, and then the tumor was segregated and weighed [17]. The tumor inhibitory ratio was calculated by the following formula:

$$\text{Tumor inhibitory ratio}\,(\%) = [(W_{\text{Control}} - W_{\text{Treated}})\,/\,W_{\text{Control}}] \times 100\%$$

W_{Treated} and W_{Control} were the average tumor weight of the treated and control mice, respectively.

Statistical analyses

All data in different experimental groups were expressed as mean ± standard error of the mean. These data shown in the study were obtained in at least three independent experiments. Statistical analyses were conducted using an unpaired, two-tailed Student's *t*-test. All comparisons are made relative to untreated controls (significance of difference is indicated as *$P < 0.05$ and **$P < 0.01$).

Results

FV-429 inhibits cell viability in HepG2 cells

To investigate the inhibitory effect of FV-429 on HepG2 cells, cell viability was assessed by MTT assay after incubation with increasing concentrations of FV-429 for 24 h. As showed in Fig. 1b, in a concentration-dependent manner, the viability of HepG2 cell was evidently inhibited after FV-429 treatment, with IC_{50} value of 39.8 ± 1.5 μmol/l.

FV-429 inhibits the growth of transplantable tumors *in vivo*

To evaluate the antitumor effect of FV-429 *in vivo*, we established a mice model bearing inoculated Heps tumor. After the 9-day treatment, FV-429 (40, 20, and 10 mg/kg) and cyclophosphamide (20 mg/kg) showed significant inhibitory effects on the growth of inoculated Heps in mice (Table 2). The inhibitory rates were 68.45, 52.12, 44.39 and 30.81%, respectively. Meanwhile, there was no significant difference in the average weight of FV-429-treated mice compared with control mice. Nevertheless, cyclophosphamide could significantly inhibit the weight of mice.
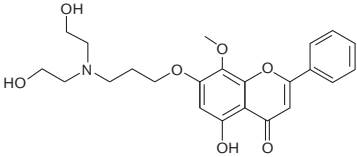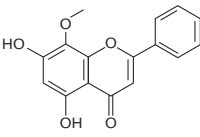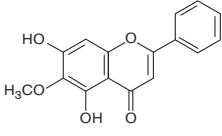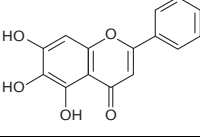
FV-429 induces apoptosis in HepG2 cells

Changes in the morphology of HepG2 cells with characteristic apoptotic appearance were observed after the treatment with FV-429. Under an inverted light microscope, the HepG2 cells treated with FV-429 were severely distorted, grew slowly, and some cells turned round in shape (Fig. 2a). Apoptotic morphology was further confirmed by using DAPI staining. Control cells emitted blue fluorescence with consistent nucleus intensity, presenting typical homogeneous distribution of chromatin in the nucleus. In contrast, cells treated with FV-429 presented the morphological features of early apoptotic cells, especially apoptotic bodies and nuclei pyknosis (Fig. 2b). FV-429-induced apoptosis in HepG2 cells was further determined using an annexin V/PI staining assay. As shown in Fig. 2c, treatment with FV-429 for 24 h increased the apoptotic death rate of cells, including both the early and the late apoptotic cells, contrasted to untreated cells. Pretreatment with NAC or Z-VAD-FMK, a caspase inhibitor, could partly inhibit the apoptosis induced by FV-429. Here, we also analyzed the specificity of FV-429 toxicity toward L02, a noncarcinoma hepatocyte, by annexin V/PI staining assay (Fig. 2d). These data suggested that the FV-429 is lower in toxicity to noncarcinoma hepatocytes *in vitro*.

Effects of FV-429 on the mitochondria of HepG2 cells

Intact mitochondrial membrane allows accumulation of JC-1 in the mitochondria, in which it will generate red fluorescent light when a critical concentration is reached. As loss of ΔΨm occurs, JC-1 cannot accumulate in the mitochondria and will remain as a monomer in the cytosol and fluoresce green light [18]. In this study, the ΔΨm change by FV-429 treatment in HepG2 cells was performed by using JC-1staining. As shown in Fig. 3a, with the increase of drug concentration, the red

Table 2 Comparison of the solubility, stability, and IC_{50} of FV-429 with wogonin, oroxylin A, or baicalein

Title	Structural formula	Freely soluble	Soluble	Sparingly soluble	Practically insoluble	Stability	IC_{50} (HepG2) (µmol/l, h)
			Solubility				
FV-429		Alcohol, methanol, acetone, ethyl acetate, glacial acetic acid	Chloroform	Water	–	Light and heat stable	40, 24
Wogonin		–	Alcohol, methanol, acetone, ethyl acetate	Chloroform, glacial acetic acid	Water	Light and heat stable	100, 48
Oroxylin A		–	Alcohol, acetone, hot benzene, ether, alkalis, glacial acetic acid	Chloroform	Water	Light and heat stable	80, 48
Baicalein		–	Alcohol, methanol, ether, acetone, ethyl acetate, hot glacial acetic acid	Chloroform, nitrobenzene	Water	Light and heat stable	100, 24

fluorescence was attenuated whereas the green fluorescence was enhanced markedly. In contrast, flow cytometric analysis also revealed that more cells became susceptible to mitochondrial membrane depolarization after FV-429 treatment, compared with the control group (Fig. 3b). Pretreatment with NAC could partly inhibit the effect of FV-429 on the ΔΨm change of HepG2 cells. However, Z-VAD-FMK, a caspase inhibitor, has little effect on the ΔΨm change induced by FV-429. To further investigate the proapoptotic effects of FV-429 on mitochondria, the levels of intracellular ROS in HepG2 cells was measured by flow cytometry. As shown in Fig. 3c, compared with control cells, the treatment of FV-429 for 24 h resulted in a conspicuous and concentration-dependent increase in ROS content, and this effect could be partly inhibited by NAC. The time-dependent level of loss of MMP and ROS generation were also analyzed (Fig. 3d and e). Data suggested that ROS generation preceded the loss of MMP.

### Effects of FV-429 on apoptotic signaling pathway
To determine the signaling pathway responsible for apoptosis induction of FV-429, the expressions of Bax, Bcl-2, and caspase-3 and caspase-9 were examined subsequently. Results showed that the expression of Bcl-2 was decreased, whereas Bax was increased after cells were treated with FV-429 for 24 h, leading to an

outstanding increase of the Bax/Bcl-2 ratio. Caspase-9 and caspase-3 were activated significantly after FV-429 treatment for 24 h in HepG2 cells and PARP cleavage was also observed, indicating that the mitochondrial pathway was involved in FV-429-induced apoptosis (Fig. 4a). Mitochondrial dysfunction could induce the translocation of proapoptotic proteins, such as cytochrome *c* and AIF, which subsequently causes a caspase-dependent or a caspase-independent apoptosis. Here, we demonstrated the translocation of cytochrome *c* and AIF induced by FV-429 using western blot analysis (Fig. 4b and c). Cyclosporin A, which inhibits mitochondrial permeability transition, could deduce the FV-429-induced loss of MMP and release of proapoptotic factor cytochrome *c*. (Fig. 4c and d). Besides this, we also found that FV-429 could dose dependently decrease the protein level of phospho-Akt in HepG2 cells without affecting the total Akt and inhibit activated NF-κB into nuclei from cytosol (Fig. 4e).

Mitogen-activated protein kinase pathway may be involved in the apoptosis induced by FV-429
As it has been reported that ROS could activate MAPK pathway and induce cell apoptosis we investigated the activation of MAPK pathway in cells treated with FV-429. These data showed that the levels of phosphorylated JNK and p38 were increased, whereas the level of phosphorylated

Fig. 2
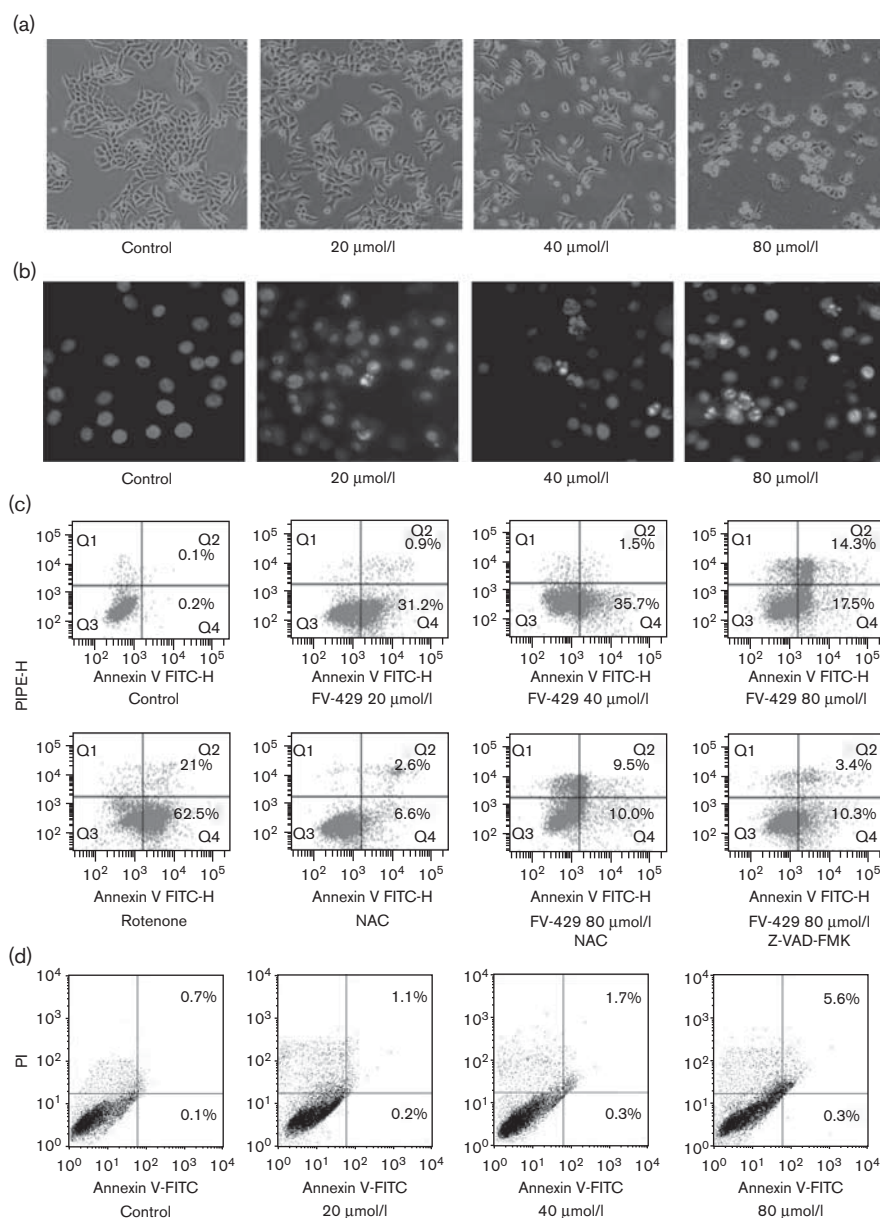
FV-429 induces apoptosis in HepG2 cells. HepG2 cells were treated with 20, 40, and 80 μmol/l of FV-429 for 24 h. (a) Morphological change of HepG2 cells was observed under an inverted light microscope (× 400). (b) Nucleolus morphological changes observed by a fluorescence microscope (× 400). Apoptotic cells are observed for apoptotic bodies and nuclei pyknosis. (c) Annexin V/propidium iodide (PI) double-staining assay of HepG2 cells. (d) Annexin V/PI double-staining assay of L02 cells. NAC, N-acetyl-L-cysteine. PIPE-H, propidium iodide of phycoerythrin-H.

extracellular receptor kinase was decreased (Fig. 5a). Pretreatment with NAC could partly reverse the activation of MAPK pathway induced by FV-429, but Z-VAD-FMK, a caspase inhibitor, has little effect on this activation (Fig. 5b). Here, we also performed annexin V/PI double-staining assay of HepG2 cells treated with FV-429 (80 μmol/l) alone or with SB203580 (P38 MAPK inhibitor) and SP600125 (JNK inhibitor). As shown in Fig. 5c, the results suggested that apoptosis induction of FV-429 could be partly inhibited by JNK and p38 inhibitors.

Discussion

As one important group of natural products derived from flavone, flavonoids are widely spread in plants, with a variety of biological activities including antimicrobial, anti-inflammatory, antimutational activities and anti-cancer effects [19]. FV-429 is a newly synthesized flavonoid with a bis(2-hydroxyethyl) amino propoxy substitution. In this study, we have provided evidence that FV-429 has potent antitumor activity by inducing a ROS–mitochondrial-mediated apoptosis.

Fig. 3

(a)

(b)

(c)

(d)

(e)
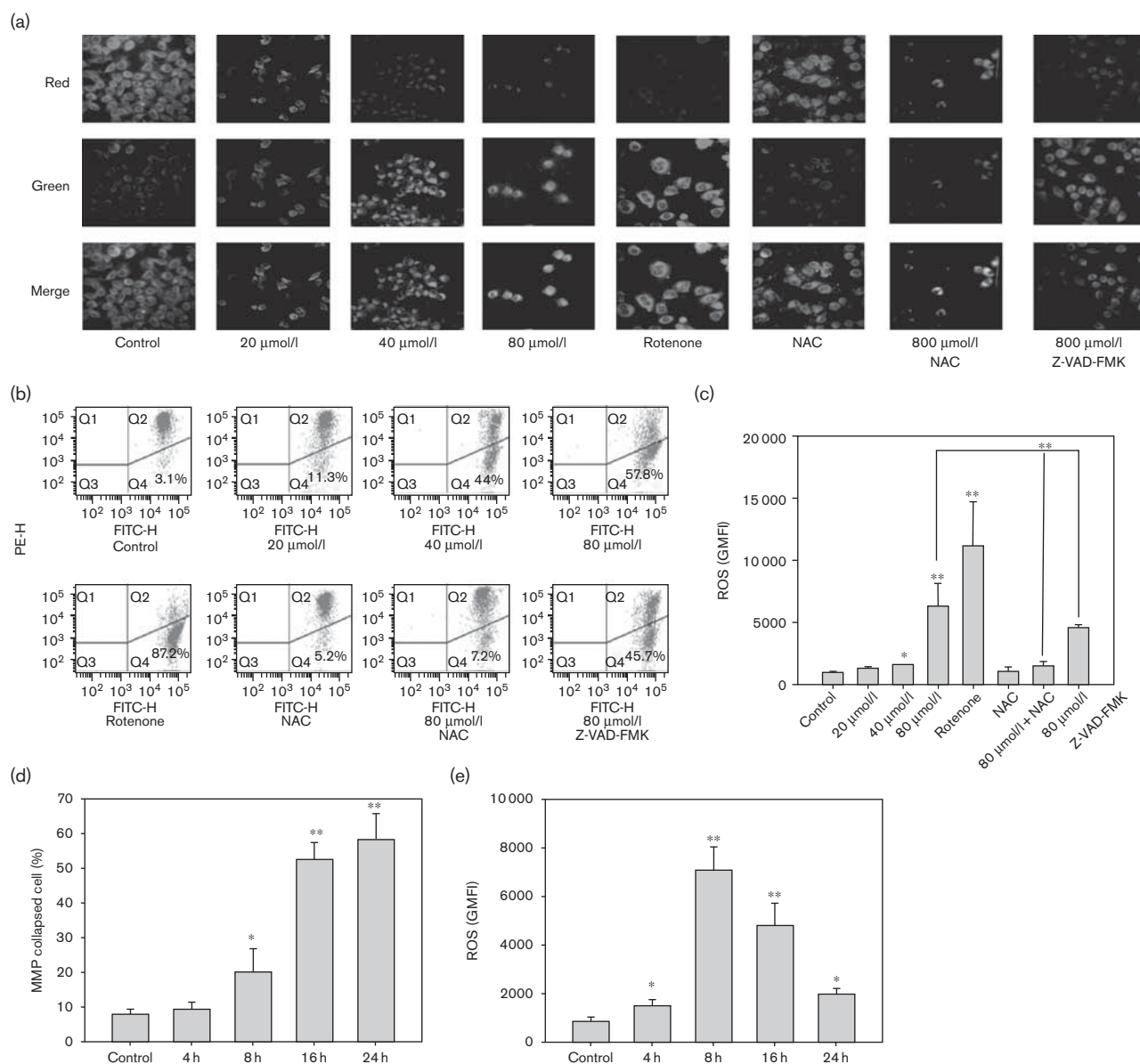
Effects of FV-429 on the mitochondria of HepG2 cells. (a and b) The change of $\Delta\Psi m$ was detected by using JC-1 staining under fluorescence microscopes and was analyzed by flow cytometry. (c) The level of intracellular reactive oxygen species (ROS) in HepG2 cells was measured by flow cytometry and was expressed as geometric mean fluorescence intensity (GMFI). (d) HepG2 cells were treated with FV-429 (80 μmol/l) for an indicated time and then the change of $\Delta\Psi m$ was analyzed by flow cytometry. (e) HepG2 cells were treated with FV-429 (80 μmol/l) for an indicated time and then level of intracellular ROS was measured by flow cytometry and expressed as GMFI. MMP, mitochondrial membrane potential; NAC, N-acetyl-L-cysteine. Results represent mean values of three experiments $\pm$ SEM, *$P < 0.05$ compared with control; **$P < 0.01$ compared with control. PE-H: phycoerythrin-H.

Here, we used a mice model bearing inoculated Heps tumor to evaluate the antitumor effect of FV-429 *in vivo*. Compared with control, FV-429 had no significant influence on the body weight in mice with Heps, whereas very significant change on them resulted from cyclophosphamide. The significant suppression of tumor growth was also observed in Heps-bearing mice. After the treatment of FV-429 (40 mg/kg), the inhibitory rate of tumor weight was 52.12%. These results suggested that

FV-429 exerted a remarkable anticancer activity *in vivo* and might be with low toxicity. On the basis of the above data, we next focussed our effort on investigating the mechanism of tumor growth repression by FV-429.

Apoptosis is characterized by a variety of morphological features, including changes in the plasma membrane such as loss of membrane asymmetry and attachment, cell shrinkage, chromatin condensation, and chromosomal

Fig. 4
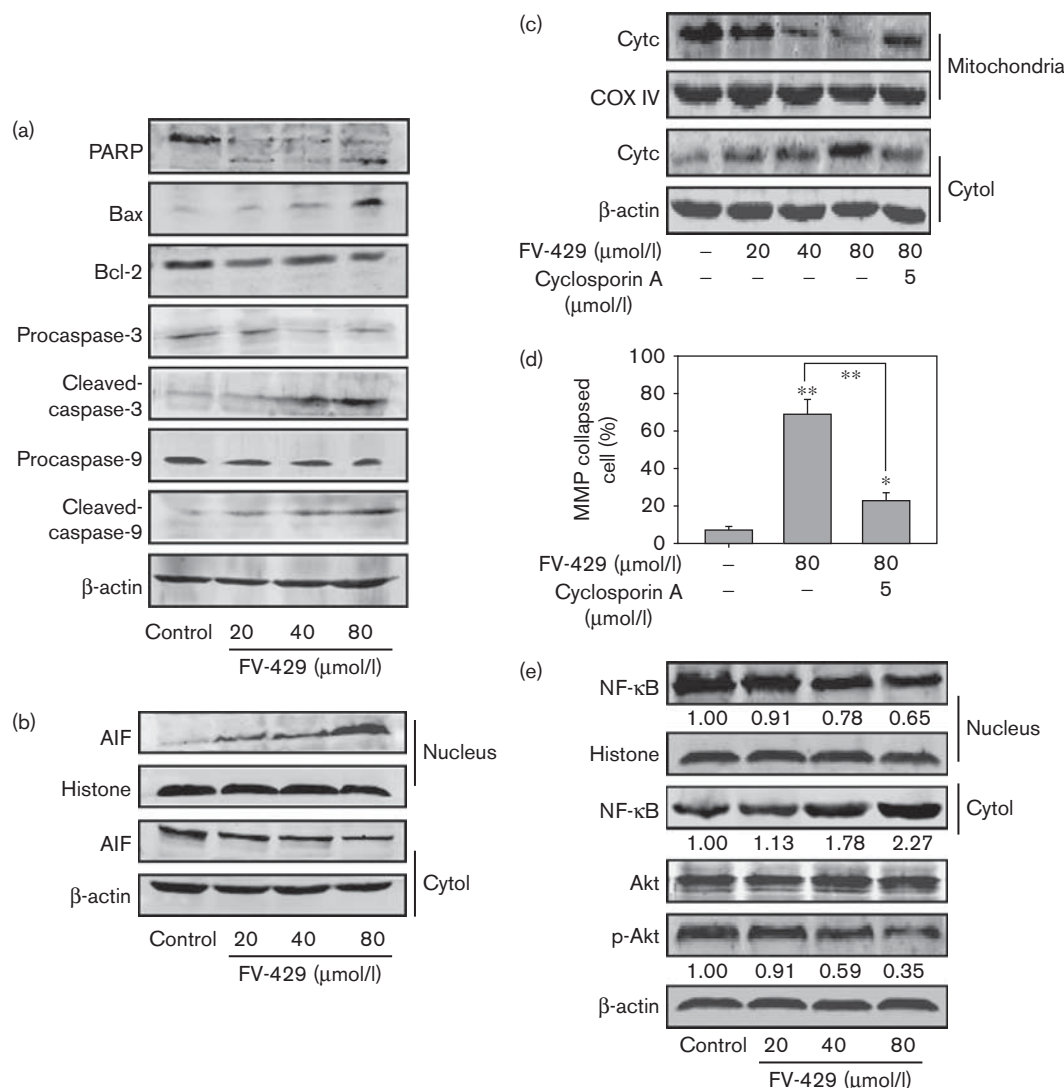
Effects of FV-429 on apoptotic signaling pathway. (a) Western blotting analysis of Bax, Bcl-2, procaspase-3 and procaspase-9, cleaved caspase-3 and caspase-9, and poly (ADP-ribose) polymerase (PARP) of HepG2 cells treated with 20, 40, and 80 µmol/l of FV-429 for 24 h. (b) The transposition of apoptotic-inducing factor (AIF) from mitochondria to nuclei was detected. (c) HepG2 cells were treated with FV-429 (20, 40, 80 µmol/l) and cyclosporin A (5 µmol/l). Cytochrome *c* in mitochondria and cytosol were identified by western blot analysis. (d) Flow cytometric analysis of the change of ΔΨm in HepG2 cells treated with FV-429 (80 µmol/l) alone or with cyclosporin A (5 µmol/l). (e) The status of NF-κB activation, Akt, and p-Akt in FV-429-treated (20, 40, 80 µmol/l) HepG2 cells were measured by western blotting analysis. The relative densitometric values are listed below each row. Results represent mean values of three experiments ± SEM, *$P < 0.05$ compared with control; **$P < 0.01$ compared with control.

DNA fragmentation [20–23]. It has been proved that mitochondria play a major role in apoptosis triggered by many stimuli, such as the loss of MMP [20,24]. Collapse of MMP is associated with translocation of cytochrome *c* and AIF, thereby activating the caspase–cascade system and a caspase-independent apoptosis [12]. Cytochrome *c*, once released, forms an apoptosome with apoptotic protease-activating factor 1 and procaspase-9 in the presence of deoxyadenosine triphosphate, resulting in the activation of caspase-9. The active subunit of caspase-9 further activates downstream procaspase-3. At the execution phase of apoptosis, caspase-3 is believed to be

an important cell apoptosis-inducing protease that cleaves PARP and other vital proteins [25]. AIF, a caspase-independent death effector, causes chromatin condensation, phosphatidylserine externalization, and large-scale DNA fragmentation when translocating from the mitochondrial intermembrane space to the nucleus [26]. In this study, we showed that FV-429 could obviously induce the collapse of MMP in HepG2 cells, and the subsequent translocation of AIF and cytochrome *c* and the activation of the caspase–cascade system were also found. Z-VAD-FMK, a caspase inhibitor, was used here and the apoptosis induced by FV-429 was partly

Fig. 5
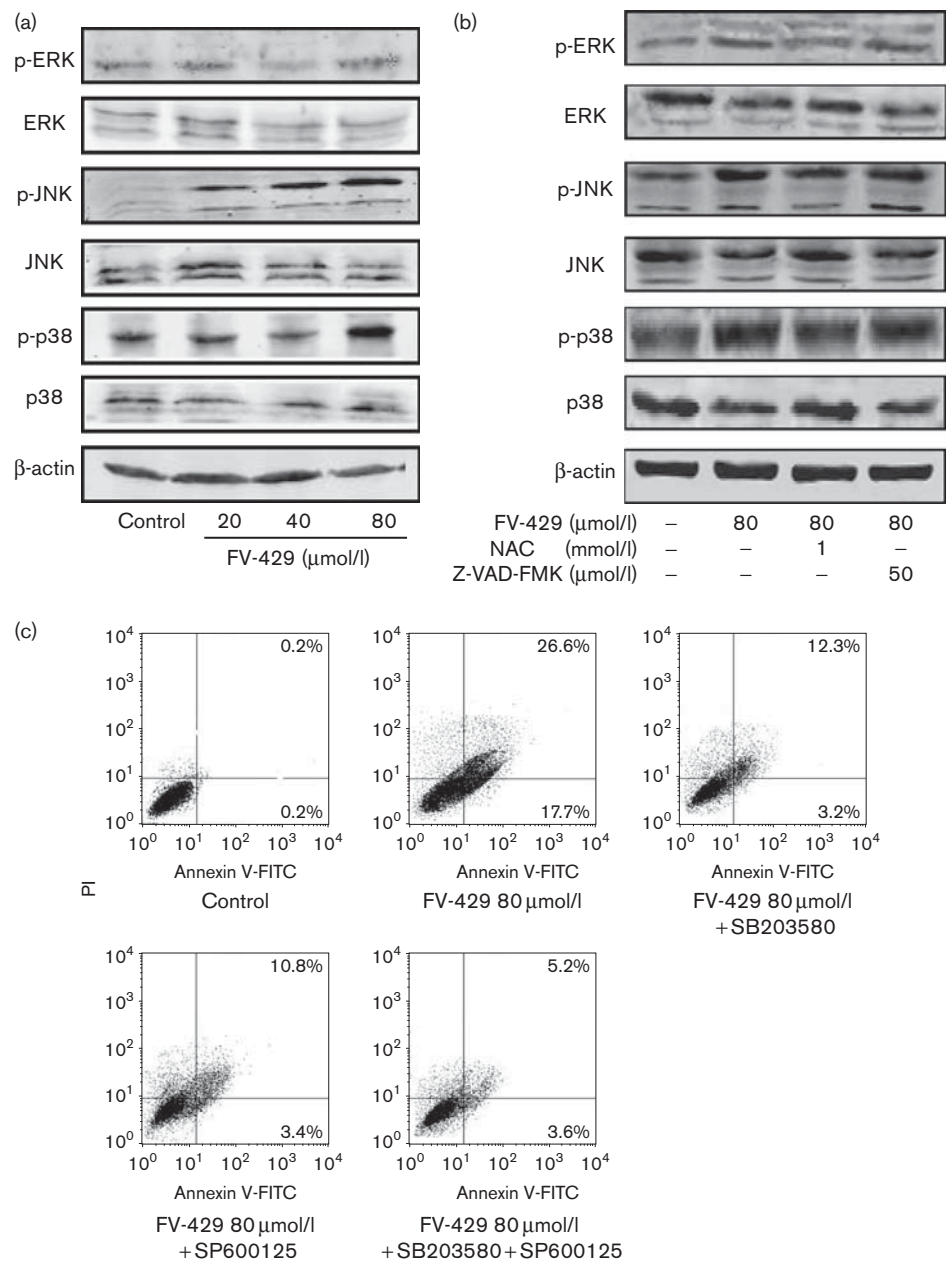
Mitogen-activated protein kinases (MAPK) pathway may be involved in the apoptosis induced by FV-429. (a) Cells were treated with FV-429 (20, 40, and 80 μmol/l) for 24 h and the expressions of extracellular receptor kinase (ERK) 1/2, p-ERK1/2, c-Jun N-terminal kinase (JNK), p-JNK, p38, and p-p38 were identified by western blot analysis. (b) Cells were treated with FV-429 (80 μmol/l) alone or with N-acetyl-L-cysteine (NAC, 1 mmol/l) and Z-VAD-FMK (50 μmol/lfor 24 h. Then expression of ERK1/2, p-ERK1/2, JNK, p-JNK, p38, and p-p38 were identified by western blot analysis. (c) Cells were treated with FV-429 (80 μmol/l) alone or with SB203580 (25 μmol/l, p38 MAPK inhibitor) and SP600125 (25 μmol/l, JNK inhibitor), then the apoptotic rates were identified by flow cytometry.

inhibited. This suggested that the apoptosis induced by FV-429 was largely caspase dependent, and the collapse of MMP may be upstream of this apoptosis pathway.

It has been reported that the accumulation of ROS is associated with the collapse of MMP and the subsequent oxidative damage to the mitochondrial membranes

impairs the membrane integrity, leading to cytochrome c release, caspase activation, and apoptosis [27,28]. Moreover, ROS was recently shown to induce apoptosis by regulating phosphorylation and activation of the MAPK pathways, resulting in an increased proapoptotic protein levels and decreased antiapoptotic protein expression, with subsequent loss of MMP and cell death [29,30]. Our

study showed that FV-429-induced apoptosis involves ROS generation. Furthermore, we attempted to investigate whether the MAPK pathways were involved in FV-429-treated HepG2 cells. The results suggested that FV-429 is an activator of MAPK including extracellular receptor kinases, JNK, and p38 kinase in HepG2 cells. Pretreatment with NAC could partly inhibit the accumulation of ROS, the activation of MAPK pathway, and the apoptosis induced by FV-429. Further study suggested that the activation of MAPK pathway is essential for FV-429-induced apoptosis, and may have occurred between the accumulation of ROS and the activation of caspase. Previous study reported that flavonoids could induce apoptosis through downregulating defensive pathways, such as PI3K/Akt and NF-κB [31]. Here, we also found that FV-429 could dose dependently inhibit the activation of PI3K/Akt and NF-κB pathways. This inhibition effect may also have contributed to FV-429-induced apoptosis in HepG2 cells.

On the basis of all those results, we come to a conclusion that FV-429 exhibited potent antitumor effects in the hepatic carcinoma cell both *in vitro* and *in vivo*, in which apoptosis may be involved. Further data showed that FV-429 could induce the increase of Bax/Bcl-2 ratio, collapse of the MMP, and the subsequent activation of the caspase cascade. The accumulation of ROS and the activation of JNK and p38 MAPK pathways induced by FV-429 were also observed. Besides these, the inhibition of PI3K/Akt and NF-κB pathways may also have contributed to FV-429-induced apoptosis. Whatever our findings provide a new candidate compound, FV-429, for its potential use in liver cancer therapy.

Acknowledgements

Conflicts of interest
None declared.

References

1 Shi LX, Ma R, Lu R, Xu Q, Zhu ZF, Wang L, *et al.* Reversal effect of tyroservatide (YSV) tripeptide on multi-drug resistance in resistant human hepatocellular carcinoma cell line BEL-7402/5-FU. *Cancer Lett* 2008; **269**:101–110.

2 Bruix J, Sherman M, Llovet JM, Beaugrand M, Lencioni R, Burroughs AK, *et al.* Clinical management of hepatocellular carcinoma: conclusions of the Barcelona-2000 EASL conference. European Association for the Study of the Liver. *J Hepatol* 2001; **35**:421–430.

3 Giglia JL, Antonia SJ, Berk LB, Bruno S, Dessureault S, Finkelstein SE. Systemic therapy for advanced hepatocellular carcinoma: past, present, and future. *Cancer Control* 2010; **17**:120–129.

4 Aiyegoro OA, Okoh AI. Phytochemical screening and polyphenolic antioxidant activity of aqueous crude leaf extract of *Helichrysum pedunculatum*. *Int J Mol Sci* 2009; **10**:4990–5001.

5 Wang W, Guo Q, You Q, Zhang K, Yang Y, Yu J, *et al.* Involvement of Bax/Bcl-2 in wogonin-induced apoptosis of human hepatoma cell line SMMC-7721. *Anticancer Drugs* 2006; **17**:797–805.

6 Wang W, Guo QL, You QD, Zhang K, Yang Y, Yu J, *et al.* The anticancer activities of wogonin in murine sarcoma S180 both *in vitro* and *in vivo*. *Biol Pharm Bull* 2006; **29**:1132–1137.

7 Gao Y, Lu N, Ling Y, Chen Y, Wang L, Zhao Q, *et al.* Oroxylin A inhibits angiogenesis through blocking vascular endothelial growth factor-induced KDR/Flk-1 phosphorylation. *J Cancer Res Clin Oncol* 2008; **136**:667–675.

8 Liu W, Mu R, Nie FF, Yang Y, Wang J, Dai QS, *et al.* MAC-related mitochondrial pathway in oroxylin-A-induced apoptosis in human hepatocellular carcinoma HepG2 cells. *Cancer Lett* 2009; **284**:198–207.

9 Elchuri S, Oberley TD, Qi W, Eisenstein RS, Jackson Roberts L, Van Remmen H, *et al.* CuZnSOD deficiency leads to persistent and widespread oxidative damage and hepatocarcinogenesis later in life. *Oncogene* 2005; **24**:367–380.

10 Benz CC, Yau C. Ageing, oxidative stress and cancer: paradigms in parallax. *Nat Rev Cancer* 2008; **8**:875–879.

11 Kulkarni GV, Lee W, Seth A, McCulloch CA. Role of mitochondrial membrane potential in concanavalin A-induced apoptosis in human fibroblasts. *Exp Cell Res* 1998; **245**:170–178.

12 Jin YH, Yim H, Park JH, Lee SK. Cdk2 activity is associated with depolarization of mitochondrial membrane potential during apoptosis. *Biochem Biophys Res Commun* 2003; **305**:974–980.

13 Sakon S, Xue X, Takekawa M, Sasazuki T, Okazaki T, Kojima Y, *et al.* NF-kappaB inhibits TNF-induced accumulation of ROS that mediate prolonged MAPK activation and necrotic cell death. *EMBO J* 2003; **22**:3898–3909.

14 Wang M, Zhang L, Han X, Yang J, Qian J, Hong S, *et al.* Atiprimod inhibits the growth of mantle cell lymphoma *in vitro* and *in vivo* and induces apoptosis via activating the mitochondrial pathways. *Blood* 2007; **109**:5455–5462.

15 Liu T, Hannafon B, Gill L, Kelly W, Benbrook D. Flex-Hets differentially induce apoptosis in cancer over normal cells by directly targeting mitochondria. *Mol Cancer Ther* 2007; **6**:1814–1822.

16 Bobyleva V, Pazienza TL, Maseroli R, Tomasi A, Salvioli S, Cossarizza A, *et al.* Decrease in mitochondrial energy coupling by thyroid hormones: a physiological effect rather than a pathological hyperthyroidism consequence. *FEBS Lett* 1998; **430**:409–413.

17 Guo QL, Wu MS, Chen Z. Comparison of antitumor effect of recombinant L-asparaginase with wild type one *in vitro* and *in vivo*. *Acta Pharmacol Sin* 2002; **23**:946–951.

18 DeRosier LC, Buchsbaum DJ, Oliver PG, Huang ZQ, Sellers JC, Grizzle WE, *et al.* Combination treatment with TRA-8 anti death receptor 5 antibody and CPT-11 induces tumor regression in an orthotopic model of pancreatic cancer. *Clin Cancer Res* 2007; **13**:5535s–5543s.

19 Kidd PM. Bioavailability and activity of phytosome complexes from botanical polyphenols: the silymarin, curcumin, green tea, and grape seed extracts. *Altern Med Rev* 2009; **14**:226–246.

20 Reed JC. Mechanisms of apoptosis. *Am J Pathol* 2000; **157**:1415–1430.

21 Finkel E. Does cancer therapy trigger cell suicide? *Science* 1999; **286**:2256–2258.

22 Sun SY, Hail N Jr, Lotan R. Apoptosis as a novel target for cancer chemoprevention. *J Natl Cancer Inst* 2004; **96**:662–672.

23 Reed JC. Bcl-2 family proteins: regulators of apoptosis and chemoresistance in hematologic malignancies. *Semin Hematol* 1997; **34**:9–19.

24 Wang X. The expanding role of mitochondria in apoptosis. *Genes Dev* 2001; **15**:2922–2933.

25 Wang XH, Jia DZ, Liang YJ, Yan SL, Ding Y, Chen LM, *et al.* Lgf-YL-9 induces apoptosis in human epidermoid carcinoma KB cells and multidrug resistant KBv200 cells via reactive oxygen species-independent mitochondrial pathway. *Cancer Lett* 2007; **249**:256–270.

26 Xie CY, Yang W, Li M, Ying J, Tao SJ, Li K, *et al.* Cell apoptosis induced by delta-elemene in colorectal adenocarcinoma cells via a mitochondrial-mediated pathway. *Yakugaku Zasshi* 2009; **129**:1403–1413.

27 Kamata H, Manabe T, Kakuta J, Oka S, Hirata H. Multiple redox regulation of the cellular signaling system linked to AP-1 and NFkappaB: effects of *N*-acetylcysteine and H2O2 on the receptor tyrosine kinases, the MAP kinase cascade, and IkappaB kinases. *Ann N Y Acad Sci* 2002; **973**:419–422.

28 Ruffels J, Griffin M, Dickenson JM. Activation of ERK1/2, JNK and PKB by hydrogen peroxide in human SH-SY5Y neuroblastoma cells: role of ERK1/2 in H2O2-induced cell death. *Eur J Pharmacol* 2004; **483**:163–173.

29 Zhang Y, Chen F. Reactive oxygen species (ROS), troublemakers between nuclear factor-kappaB (NF-kappaB) and c-Jun NH(2)-terminal kinase (JNK). *Cancer Res* 2004; **64**:1902–1905.

30 Kuo PL, Chen CY, Hsu YL. Isoobtusilactone A induces cell cycle arrest and apoptosis through reactive oxygen species/apoptosis signal-regulating kinase 1 signaling pathway in human breast cancer cells. *Cancer Res* 2007; **67**:7406–7420.

31 Aggarwal BB, Shishodia S. Molecular targets of dietary agents for prevention and therapy of cancer. *Biochem Pharmacol* 2006; **71**:1397–1421.